Supporting Information

An enhanced centrifugation-assisted lateral flow immunoassay for the point-of-care detection of protein biomarkers

Minjie Shen,[a] Nan Li,[a] Ying Lu,[a, c] Jing Cheng[a, b, c*] and Youchun Xu[a, c*]

[a] State Key Laboratory of Membrane Biology, Department of Biomedical Engineering, School of Medicine, Tsinghua University, Beijing 100084, China.

[b] Center for Precision Medicine, West China Hospital, Sichuan University, Chengdu, 610041, China.

[c] National Engineering Research Center for Beijing Biochip Technology, Beijing 102206, China.

*Correspondence should be addressed to J.C. (jcheng@tsinghua.edu.cn) or Y.X. (xyc2012@tsinghua.edu.cn).

Tel: (86)-10-62796071.

Supporting Information Contents:

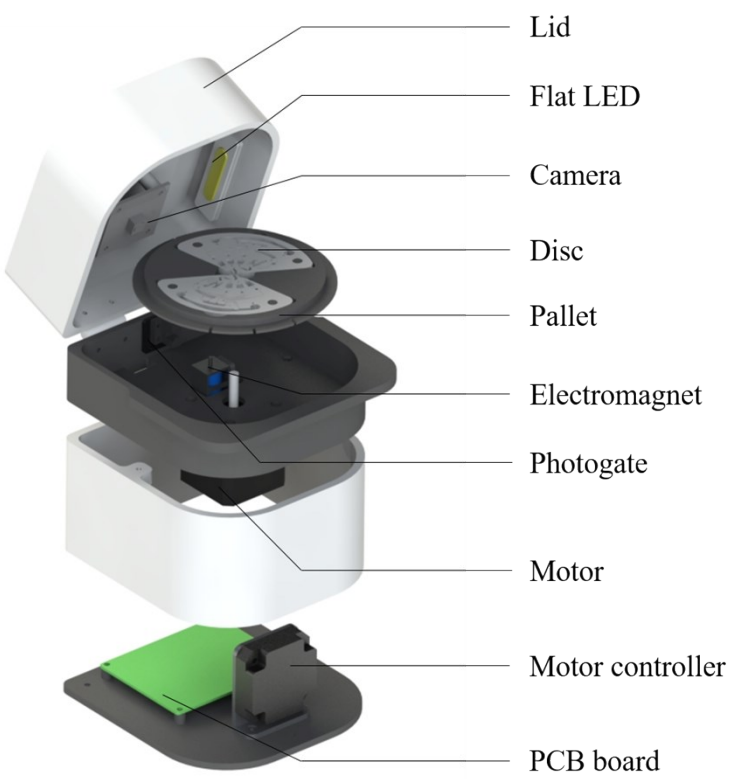

Figure S1. Schematic of the supporting device for ECLFIA.

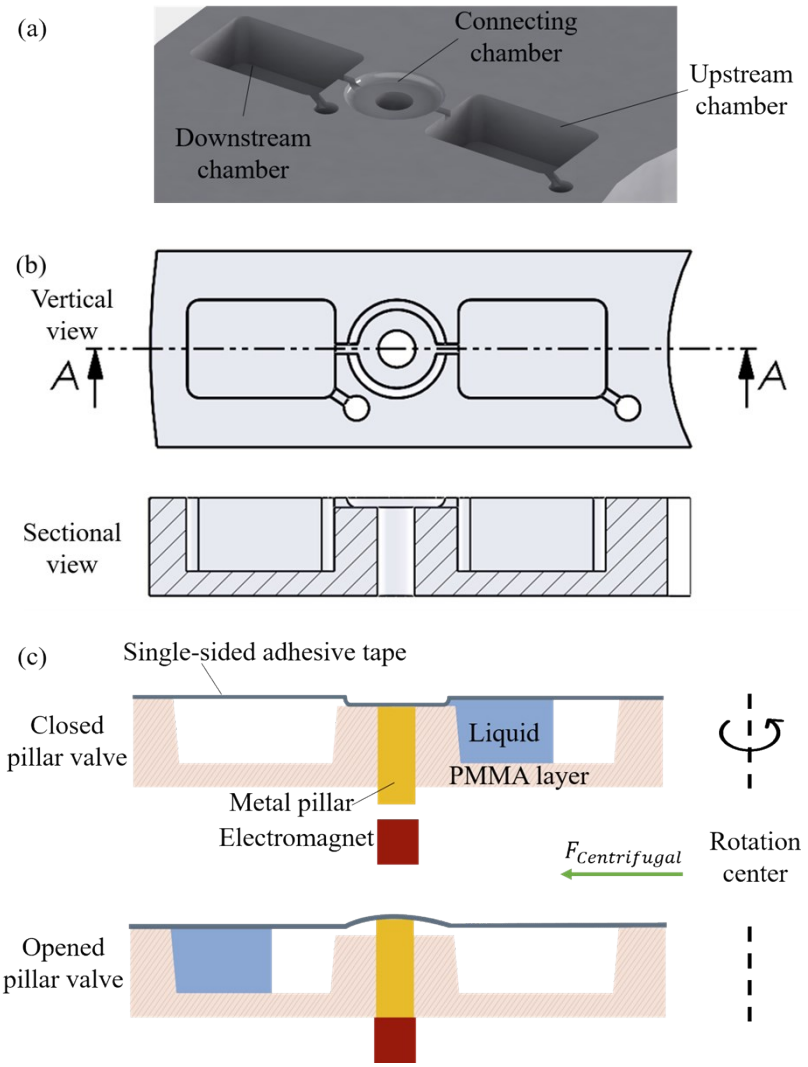

Figure S2. Working principle of the pillar valve. (a) Schematic of the chambers in a pillar valve. (b) Vertical view and sectional view of a disc with a pillar valve. (c) Schematics of the closed and opened pillar valves in sectional views of the disc. The connecting chamber is sealed before the pillar valve is opened. During centrifugation, the liquid in the upstream chamber cannot be transferred to the downstream chamber due to the obstruction of the sealed connecting chamber. The adhesive tape is capable to stand the high rotation speed (>4200 rpm) for a long time (>15 min) to avoid liquid leakage. Once the electromagnet is triggered, the pillar will be lifted up and the tape will be separated from the PMMA layer to open the pillar valve. Then, the liquid can

be transferred to the downstream chamber under the centrifugal force, and no liquid leakage occurs through the pillar hole due to the overwhelming centrifugal force than the gravity during liquid transfer and the interference fit between the through-hole and the pillar.

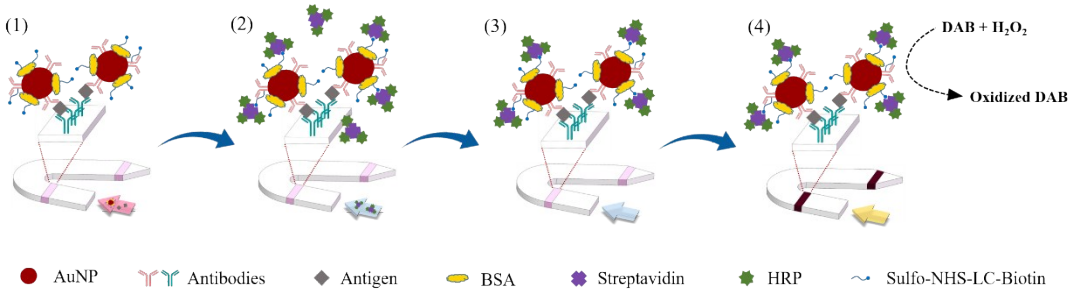

Figure S3. Schematic showing the process of ECLFIA. (1) Antibody-antigen conjugation. (2) Biotin-streptavidin conjugation. (3) Washing. (4) HRP-catalyzed signal amplification.

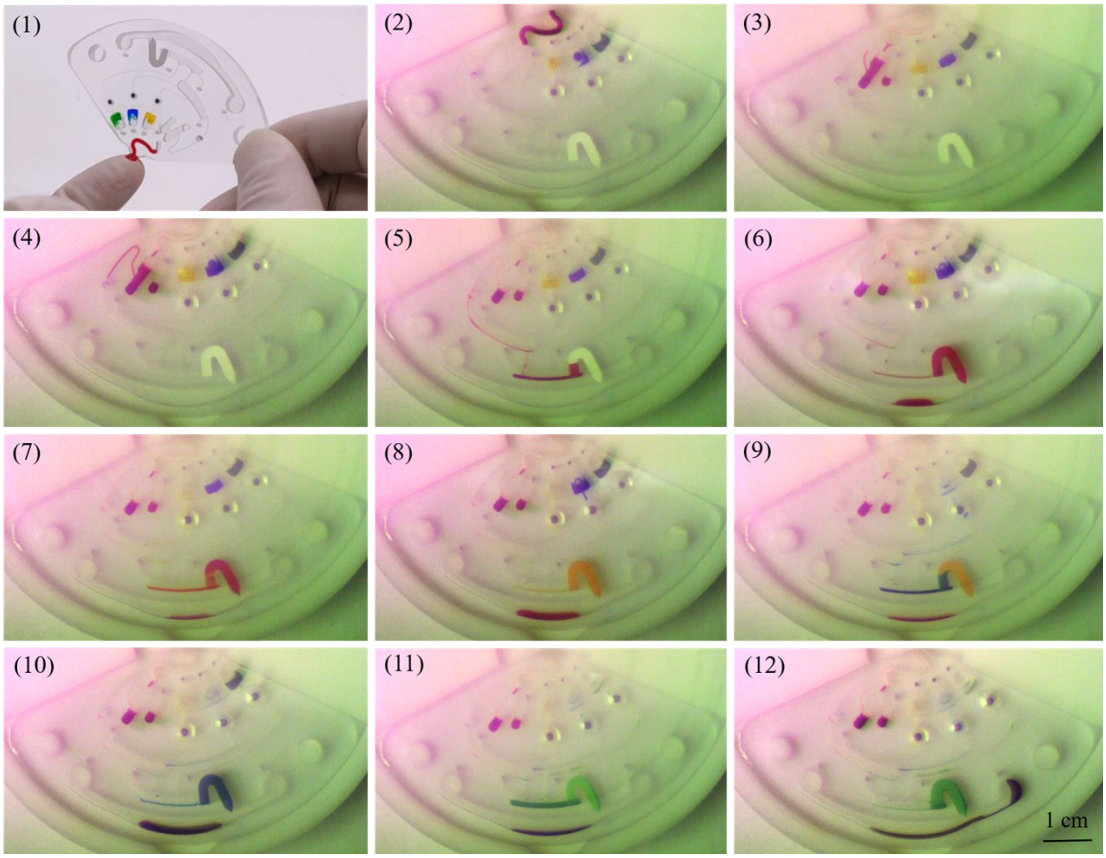

Figure S4. Photographic images of the ECLFIA workflow. (1) Sample aspiration. (2) Disc placement on the centrifugal pallet. (3) Sample metering and blood cell separation. (4) Liquid filling the microchannel of the siphon valve. (5) Liquid transfer and lateral flow reaction of antibody-antigen conjugation. (6) Completion of step 5 and opening the pillar valve No. 1 (the left one). (7) Lateral flow reaction of biotin-streptavidin conjugation. (8) Completion of step 7 and opening the pillar valve No. 2 (the middle one). (9) Lateral flow process of washing. (10) Completion of step 9 and opening the pillar valve No. 3 (the right one). (11) DAB substrate transfer. (12) Catalytic reaction.

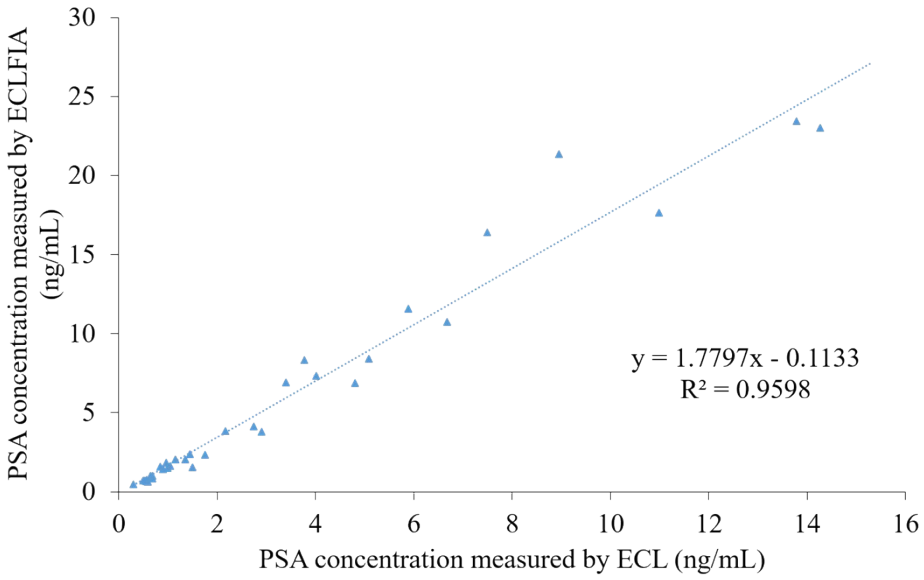

Figure S5. Correlation between PSA concentrations in blood samples measured by ECLFIA and ECL. The PSA concentrations measured by ECLFIA were all calculated using the standard curve fitted by the signal amplification results.

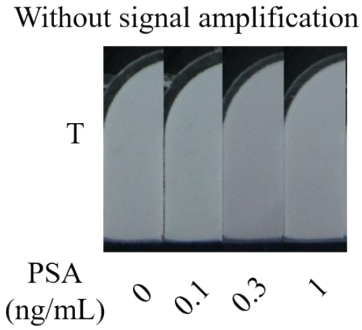

Figure S6. Results of ECLFIA without signal amplification of PSA at concentrations of 1 ng/mL and below.

Table S1. Summary of the analytical performances for detecting PSA by LFIA or microfluidic devices.

Detection	LOD	Time	POC*	Ref.
Silver and gold enhancement LFIA	0.1 ng/mL	20 min	No	[1]
Upconversion nanoparticle based LFIA	0.089 ng/mL	30 min	Yes	[2]
Centrifugation assisted LFIA	0.067 ng/mL	45 min	Yes	[3]
Fluoropolymer microfluidic device	0.08 ng/mL	22 min	No	[4]
Reduced graphene oxide/BiFeO3 nanohybrids-based photoelectrochemical sensing system	0.31 pg/mL	> 1.5 h	No	[5]
Microcapillary film based microfluidic ELISA	< 0.9 ng/mL	15 min	Yes	[6]
SERS-based microdroplet sensor	< 0.1 ng/mL	-	No	[7]
Sigle bead trapping and acoustic mixing integrated microfluidic platform	0.028 ng/mL	20 min	No	[8]
Microfluidic electrochemical sensing	0.84 pg/mL	> 1.5 h	No	[9]
Aptamer probe based microdroplet	0.035 ng/mL	> 3 h	No	[10]
Enhanced centrifugation-assisted LFIA	0.028 ng/mL	15 min	Yes	In this study

*POC status is evaluated according to the sample preparation, automation and bulk of the device.

References

1 M. O. Rodriguez, L. B. Covian, A. C. Garcia and M. C. Blanco-Lopez, *Talanta*, 2016, **148**, 272–278.

2 H. He, B. Liu, S. Wen, J. Liao, G. Lin, J. Zhou and D. Jin, *Anal. Chem.*, 2018, **90**, 12356–12360.

3 M. Shen, Y. Chen, Y. Zhu, M. Zhao and Y. Xu, *Anal. Chem.*, 2019, **91**, 4814–4820.

4 A. I. Barbosa, P. Gehlot, K. Sidapra, A. D. Edwards and N. M. Reis, *Biosens. Bioelectron.*, 2015, **70**, 5–14.

5 Q. Zhou, Y. Lin, K. Zhang, M. Li and D. Tang, *Biosens. Bioelectron.*, 2018, **101**, 146–152.

6 A. I. Barbosa, A. P. Castanheira, A. D. Edwards and N. M. Reis, *Lab Chip*, 2014, **14**, 2918–2928.

7 R. Gao, Z. Cheng, A. J. deMello and J. Choo, *Lab Chip*, 2016, **16**, 1022–1029.

8 H. Chen, C. Chen, S. Bai, Y. Gao, G. Metcalfe, W. Cheng and Y. Zhu, *Nanoscale*, 2018, **10**, 20196–20206.

9 S. Chen, Z. Wang, X. Cui, L. Jiang, Y. Zhi, X. Ding, Z. Nie, P. Zhou and D. Cui, *Nanoscale Res. Lett.*, 2019, **14**, 71.

10 Y. Zhang, W. Ye, C. Yang and Z. Xu, *Talanta*, 2019, **205**, 120096.